Journal of Power Sources 271 (2014) 382–391

Contents lists available at ScienceDirect

Journal of Power Sources

journal homepage: www.elsevier.com/locate/jpowsour

Structural analysis and experimental characterization of cylindrical lithium-ion battery cells subject to lateral impact

Ilya Avdeev*, Mehdi Gilaki

Department of Mechanical Engineering, College of Engineering & Applied Science, University of Wisconsin-Milwaukee, 3200 N. Cramer Street, EMS 975, Milwaukee, WI 53211-3029, United States

HIGHLIGHTS

- We report on modeling response of cylindrical lithium-ion battery cells to impact.
- The proposed model was validated through experimental testing.
- Two homogenization methods for the jellyroll were developed.
- Experimental results showed a very good agreement with simulations.

ARTICLE INFO

Article history:
Received 2 April 2014
Received in revised form
29 July 2014
Accepted 3 August 2014
Available online 14 August 2014

Keywords:
Lithium-ion battery
Impact
Explicit finite element analysis
Homogenization
Experiments

ABSTRACT

We report on modeling mechanical response of cylindrical lithium-ion battery cells that are commonly used in automotive applications when subjected to impact testing. The developed homogenized model that accurately captures mechanical response of a cell to lateral crash is reported. The proposed model was validated using static and dynamic experimental testing. Highly nonlinear mechanical deformations of the cells were captured experimentally using a high-speed camera and later characterized through computer tomography. Numerically, we have investigated the feasibility of using explicit finite element code for accurate modeling of impact on one cell, so it can be used for an entire battery pack that consists of hundreds or thousands of cells. In this study, we have developed and compared two homogenization methods for the jellyroll in a cylindrical lithium-ion battery cell. Homogenization was conducted in a lateral/radial direction. Based on the results of the homogenization, the material model utilizing crushable foam constitutive behavior was then developed for simulations. Experimental results showed a very good agreement with simulations, thus validating the proposed approach and giving us confidence to move forward with the crush simulations of an entire battery pack. Zones of potential electric shortages were determined based on the experiments and simulations.

1. Introduction

Increased usage of lithium-ion batteries in automotive applications makes it necessary to understand their mechanical behavior under extreme loading conditions, such as mechanical impact. One of the key design aspects of any energy storage system, including batteries, is safety, which can be improved by: (a) reducing the probability of an event and (b) lessening the severity of the outcome should an event occur [1]. The current study is part of a project on improving the crash safety of lithium-ion batteries. There have been some studies on failure modes, fault tree analysis, safety and reliability of lithium based batteries [2–5]. In the case of lithium-ion batteries, thermal stability is probably the most important parameter that affects safety in cells, modules and battery packs [6]. Although various safety mechanisms have been implemented in individual lithium-ion cells as well as entire battery packs based on the thermal state of the battery [7,8], there is still a need for better understanding of battery response to extreme loading, which increases a risk of short circuits and the following thermal runaway or fire. One of the biggest challenges in the structural analysis of cylindrical battery cells is a treatment of the jellyroll's mechanical response. A jellyroll consists of hundreds of thin anode, cathode and separator layers wrapped around a center pin. It is a three-dimensional heterogeneous cylindrical structure

* Corresponding author. Tel.: +1 (414) 229 6949; fax: +1 (414) 229 6958.
E-mail addresses: avdeev@uwm.edu, ilya.avdeev@gmail.com (I. Avdeev).

http://dx.doi.org/10.1016/j.jpowsour.2014.08.014
0378-7753/

that exhibits anisotropic behavior in axial and transverse directions. This anisotropy can be attributed to the laminated nature of the jellyroll as well as to the fact that the layers in the laminate are not bonded.

Several methods of modeling jellyrolls have been reported in the literature. One way to treat the material behavior of the roll is by representing it as a laminated composite structure. Chatiri et al. [9] did an assessment of the LS-DYNA layered thick shell formulation for thick composite applications to decrease the solution time and still have an acceptable accuracy. However, layered thick shell formulation is not suitable for models with high aspect ratio elements and models including soft materials such as a polymer separator. Classical laminated shell theory [10] can also be used to find the homogenized material response of the jellyroll using a multilinear interpolation of the strain-stress curve [11]. There are two problems arising from using this approach: (1) focus on in-plane properties and (2) inability to account for layers not being bonded, i.e. interlayer slippage. The results obtained using laminated shell theory turn out to be much stiffer than experimentally observed jellyroll stiffness. Kim et al. studied the behavior of small cylindrical lithium-ion cells under abnormal conditions [12]. Compressive characteristics of the jellyroll were assumed to be similar to the separator material, i.e. polypropylene. Various impact and heating tests were conducted on small 18,650 commercial cells with- and without a center pin to determine conditions for the thermal runaway. Greve and Fehrenbach developed a quasi–static mechanical abuse test program with various loading conditions for large 200 mm long and 60 mm diameter cells [13]. They tracked voltage and temperature during the test and realized that when the jellyroll fails, the voltage drops and the temperature increases due to the short circuit. They also developed a finite element model using pressure dependent isotropic Raghava yield criterion as the constitutive model of the jellyroll and applied Mohr-Coulomb criterion to predict fracture inside the jellyroll. Sahraei et al. also performed several experiments on small cylindrical cells (18,650) and recorded voltage and temperature change during their tests [14]. They used stress-strain properties found from the compressive tests on pouch cells as the constitutive model for the jellyroll in cylindrical cells as both cells consisted of the same active materials. Their developed LS-DYNA finite element simulation was based on crushable foam material model as suggested by Sahraei et al. for pouch cells [15,16]. Wierzbicki and Sahraei reported a hybrid, experimental-analytical approach to find the average stress strain properties of the jellyroll in a radial direction with the assumption that the load was carried by a central rectangular part of the jellyroll under the punch [17]. They compared the stress-strain curves of commercial 18,650 cells with the results from pouch cells consisting of the same active materials.

In this investigation, compressive tests on flattened jellyrolls were conducted in order to characterize the stress-strain relation for larger cylindrical lithium-ion cells used in hybrid and electric vehicles. In addition, we have extended the virtual work method of homogenization [17] to larger cells. The experimentally obtained stress-strain curves were incorporated into the proposed explicit finite element models used to simulate crushing cell impact placed between two flat plates. In order to verify the developed FE models, experiments were conducted on cylindrical cells using a custom designed drop test apparatus. For this study, only dry cells have been tested in order to verify the homogenization method and the explicit simulations. However, the method can be applied to “live” cells with electrolyte only if serious safety provisions in place because of the risk of cell explosion or fire. Validation of the proposed approach will help us to get closer to crash simulations of an entire battery pack, which will be used to improve battery design with respect to safety.

2. Jellyroll homogenization

In this study, we have investigated commercially available 6P cylindrical lithium-ion battery cells (3.6 V/6.8 Ah, NCA/Graphite, 140 × 40 mm) manufactured by Johnson Controls, Inc. (Milwaukee, WI), which consisted of four major mechanical components (see Fig. 1): (1) a roll of active battery materials (anode-, cathode- and separator sheets) or a “jellyroll”, (2) a center hollow aluminum tube, (3) an aluminum casing and (4) a polyetherimide spacer. The cathode was made of aluminum foil coated with $LiNiCoAlO_2$ active material on both sides. The anode was made of graphite-coated copper foil, and a thin polypropylene separator sheet was used to keep them apart. Modeling each individual layer in the jellyroll during an impact is prohibitively expensive even for one cell, not to mention an entire pack. Thus, our objective was to replace the heterogeneous jellyroll with an equivalent (mechanically) homogeneous material. In order to find the homogenized material properties of the jellyroll, two experimental approaches were considered: (1) a direct compressive uniaxial test of flattened jellyroll samples and (2) homogenization using the principle of virtual work applied to cylindrical samples. The jellyroll material behavior is nonlinear due to the fact that all individual layers forming the jellyroll i.e. anode, cathode and separator, exhibit nonlinear material behavior [17–19]. Therefore, for finite element simulation purposes, a material model has to be derived that accommodates nonlinear stress-strain curves in both radial and axial directions. In this study, an isotropic material model of the jellyroll was considered. The stress strain relation found from the homogenization of the jellyroll will be incorporated in jellyroll's material model in Section 3.3.

The two prevailing impact modes on an individual cell in a battery pack are (1) axial and (2) lateral impacts (see Fig. 2). The focus of this study was on the lateral mode, which would be the dominant deformation mode during a car crash if the battery cells are vertically oriented.

2.1. Direct homogenization using flat samples

We prepared jellyroll samples by cutting an original full length jellyroll into one-inch long cylindrical samples (see Fig. 3a). The samples were then cut in a radial direction and flattened after the inner aluminum tube was removed (see Fig. 3b).

Fig. 4 depicts a flattened sample under compression between two flat rigid plates. Three samples have been tested using an Instron 3369 tension-compression machine, and load–displacement curve was recorded for loads varying from 0 kN to 52 kN (see Fig. 5). It was assumed that only the rectangular area under the plates carried the compressive load. Therefore, stress-strain curve could be easily calculated assuming a constant cross sectional area. Fig. 6 depicts the stress-strain curves derived for the flattened jellyroll samples. The concave-upward shape of the stress-strain

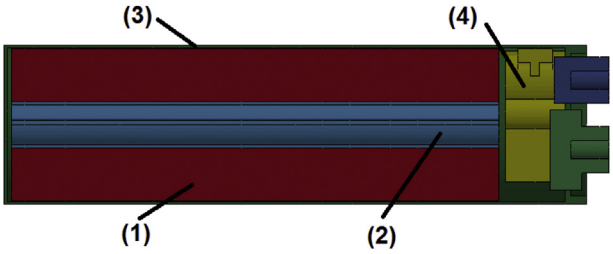

Fig. 1. Cylindrical cell components: (1) jellyroll, (2) inner tube, (3) casing and (4) spacer.

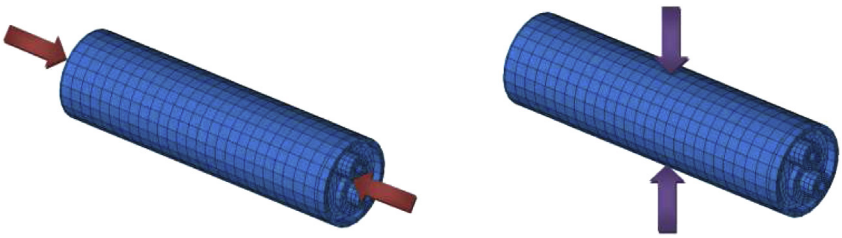

Fig. 2. Two impact modes: (1) axial direction and (2) lateral direction.

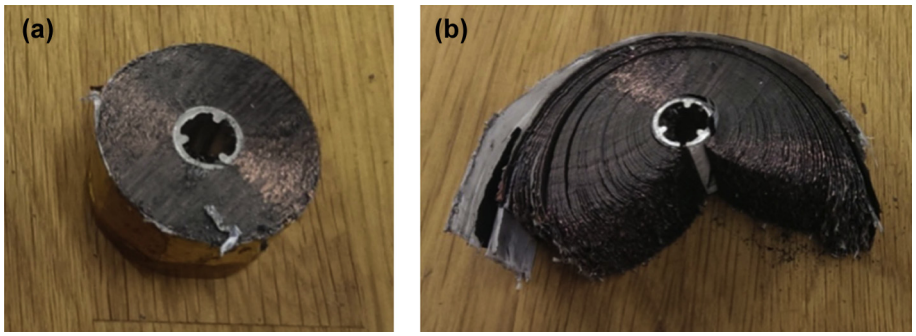

Fig. 3. (a) A jellyroll sample with the metal core and (b) a jellyroll after being cut in a radial direction.

curve suggests that there is no visible yield strength and that the load is very small for the small values of deformation. This can be attributed to the porosity of the jellyroll layers that causes the material to be very compressible with a small value of the Poisson's ratio.

2.2. Indirect homogenization using virtual work principle

The direct homogenization method, presented earlier, requires extensive cell manipulations, which might not be feasible in many lab environments, especially when dealing with “live” cells. An alternative homogenization method, based on the virtual work principle, was first proposed by Wierzbicki and Sahraei for commercial 18,650 cells [17]. In this chapter, we report on extending this method to analysis of larger cells. The results are then compared to data obtained from the direct method.

In this hybrid experimental/analytical approach, we find the stress-strain relation of the jellyroll using the cylindrical samples rather than flattened ones. It is assumed that during crushing, the compressive load is mainly carried by the central rectangular area of the jellyroll [17]. The load–displacement relation is measured for the compression test of the jellyroll between two flat plates. The virtual work principle is then used to calculate an average stress and strain in terms of the crush distance. The average stress and strain can be calculated as:

$$\sigma_{av} = \frac{2P(w)}{\pi L w} \tag{1}$$

$$\varepsilon_{av} = \frac{w}{2R} \tag{2}$$

where $P(w)$ is the crush load as a function of crush distance, w is the vertical displacement of the plates, L is the sample length in axial direction, and R is the outer radius of the sample.

Fig. 4. Flattened jellyroll sample under uniaxial compression.

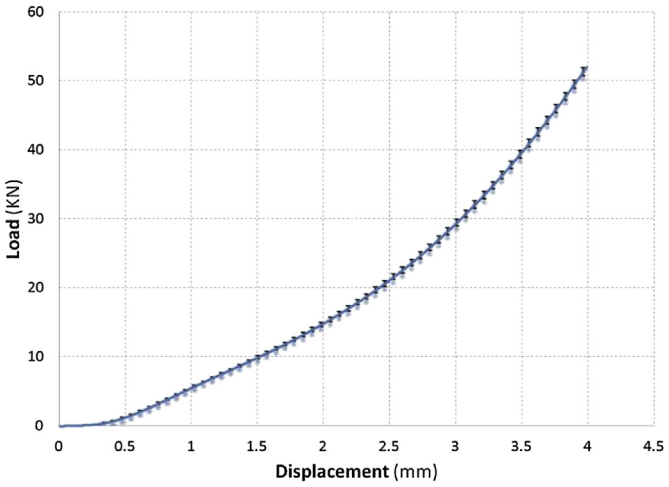

Fig. 5. Load-displacement of flattened jellyroll under compression ($n = 3$, relative SD = 1.2%).

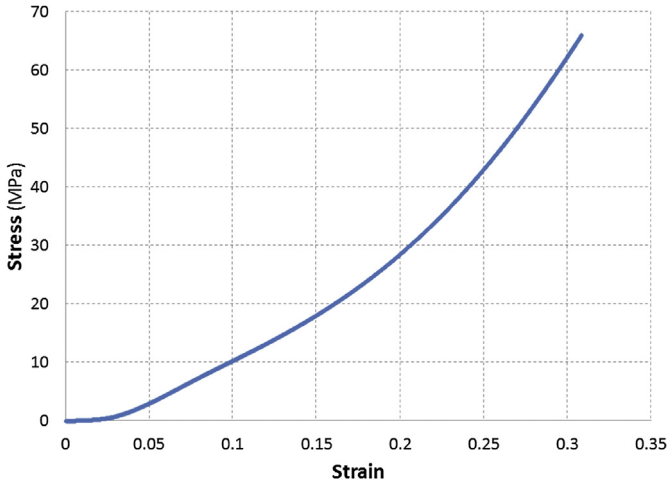

Fig. 6. Stress-strain curves for flattened jellyroll samples.

In order to be able to accurately calculate average stresses and strains in the jellyroll samples, we had to enhance the formulation proposed in Ref. [17]. In this investigation, the outer diameter of the 6P-JCI cell is about twice the size of an 18,650 cell. Consequently, the inner diameter of the aluminum core is also larger. Furthermore, during lateral compression tests of the jellyroll, it was observed that the load remains very small during the first stage of the test until the inner hole closes. At this point, load starts to increase significantly as the jellyroll carries the compressive load. In order to increase the accuracy of calculations, the flat part of the load–displacement can be discarded. This means that the starting point of the calculations changes accordingly, i.e. the initial geometry will be a smaller cylinder with diameter equal to the distance between the flat plates when the load starts to increase significantly (see Fig. 7).

In the original method for smaller cells, the cross sectional area of the cylindrical sample that carried the compressive load, S, was assumed to depend only on radius, R, and punch size, b [17]. However, for larger cells, the cross-sectional area that takes the load is also a function of r, instantaneous radius of the semi circles in the deformed jellyroll (see Fig. 8b). This assumption significantly affects the results, especially for larger strain values. Therefore, in this study the cross sectional area, S, is calculated as:

$$S = rb \tag{3}$$

The effective punch width can be calculated as:

$$b = \frac{\pi}{4}w \tag{4}$$

Therefore:

$$r = R - \frac{2b}{\pi} \tag{5}$$

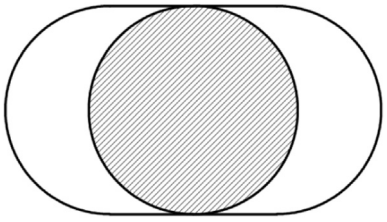

Fig. 7. Equivalent cross section for homogenized stress-strain calculations.

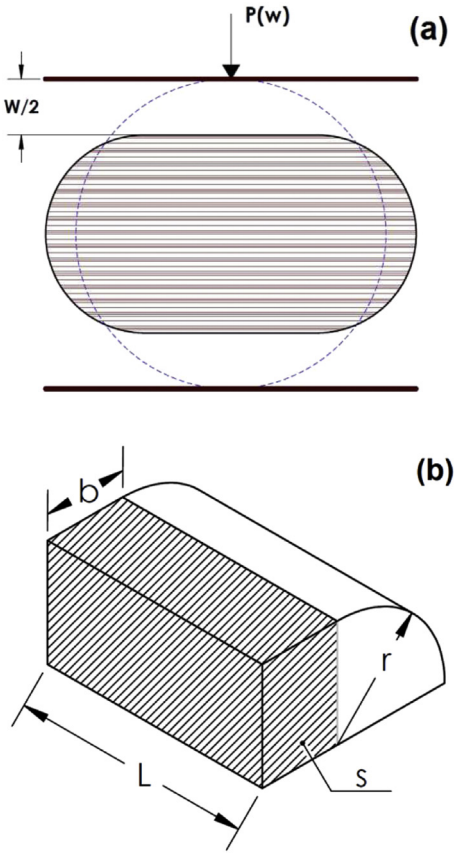

Fig. 8. Schematics of crushed samples: (a) load and displacement and (b) dimensions of the deformed jellyroll.

The effective loaded cross-section, S, can be found in terms of crush distance, w as:

$$S = rb = \frac{\pi}{4}Rw - \frac{\pi}{8}w^2 \tag{6}$$

Average strain is calculated using the following integration over time [17] is.

$$\varepsilon_{av} = \int_0^t \dot{\varepsilon}_{av}dt = \int_0^t \frac{\pi}{4}\frac{w\dot{w}}{S}dt \tag{7}$$

By substituting Eq. (6) into the above integral and performing a change of variable, the simplified average strain formula is given by.

$$\varepsilon_{av} = \int_0^w \frac{dw}{2R - w} = \ln\left(\frac{2R}{2R - w}\right) \tag{8}$$

In order to find the stress-strain relation, the crush distance must be eliminated in stress and strain equations. Solving Eq. (8) for w, we obtain:

$$w = 2R\left(1 - e^{-\varepsilon}\right) \tag{9}$$

In order to use the above calculations to estimate the homogenized mechanical properties, a set of transverse crush tests on the jellyroll pieces was performed. The jellyroll casing and the aluminum core were carefully removed after the jellyroll was cut into inch-long (in an axial direction) samples. The samples were compressed between two flat steel plates at a rate of 1.0 mm min^{-1}.

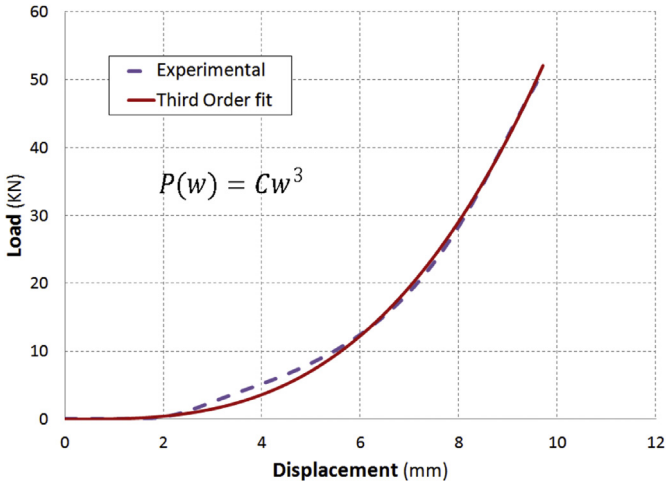

Fig. 9. Load-displacement relation and its third order interpolation.

The applied load and the plate displacement were recorded during the experiments.

The obtained load–displacement curve can be interpolated fairly accurately with a third order polynomial function as shown in (see Fig. 9):

$$P(w) = Cw^3 \tag{10}$$

where constant C equals to 57 N mm^{-3}. By substituting Eqs. (9) and (10) into Eq. (1), the average stress can be found in terms of average strain, which is depicted in Fig. 10.

$$\sigma_{av} = \frac{2C}{\pi L}\left\{2R\left(1 - e^{-\varepsilon_{av}}\right)\right\}^2 \tag{11}$$

When comparing the results of the two homogenization methods in terms of the stress-strain curve of the jellyroll material, it can be observed that curves diverge at strains exceeding 0.1, with the difference in stress being as large as 22% for strains equal to 0.3 (see Fig. 10).

The difference can be attributed to the fact that in the virtual work method uniaxial state of stress is probably not a very accurate assumption, and there will be stresses in both directions because of the integrity of the jellyroll layers. The presence of the inner hole also affects the accuracy of the results. On the other hand, the stress-strain relation found from the flattened tests is directly derived from the experiments. Besides, the issues such as biaxial state of stress and inner hole will not be available in the case of the direct method. Therefore, it is believed that the direct homogenization is more accurate than the virtual work approach.

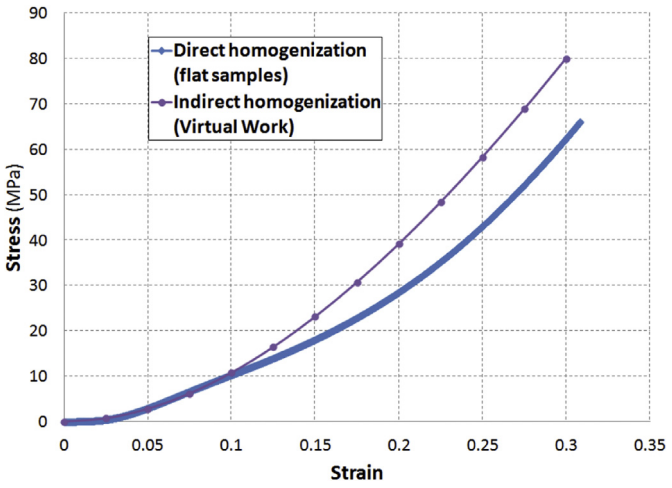

Fig. 10. Stress-strain curve comparing two homogenization methods.

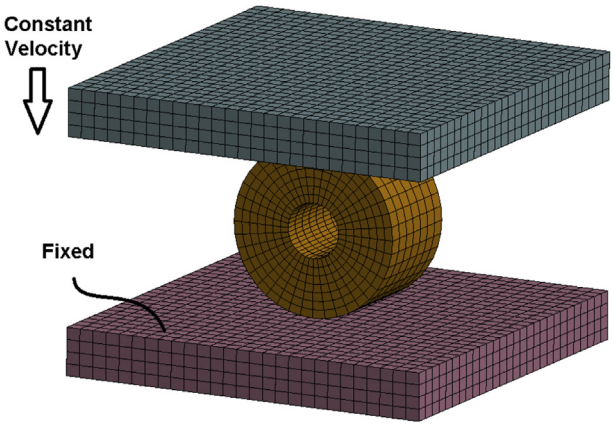

Fig. 11. 3-D Finite element model of the jellyroll transverse crushing.

2.3. Explicit finite element analysis of jellyroll crushing

In order to validate the stress-strain relation found from the direct method, an explicit 3D finite element model was created in LS-DYNA to simulate crushing the jellyroll between two rigid flat plates. The bottom plate was fixed in all directions, while the top plate was moving at a constant speed. Fig. 11 shows the finite element model of the jellyroll and the plates. The stress-strain curve found from the direct method was used as the input to the material type 63 that was the material model chosen for the jellyroll. The jellyroll sample was modeled using 1960 solid elements with one-point integration. The crushing distance of the jellyroll was recorded using the displacement of the moving plate, and the applied load was captured by the contact force between the plate and the jellyroll. As mentioned earlier, for the jellyroll crushing experiment, the first part of the load–displacement curve corresponding to small loads was removed. In order to match the staring

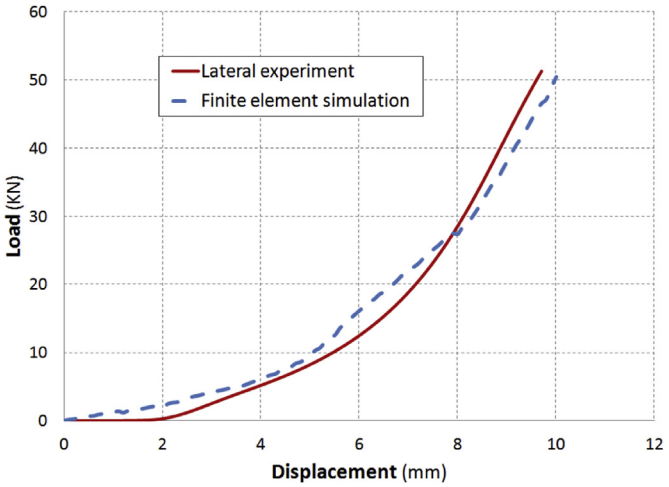

Fig. 12. Comparison of the load–displacement curves from lateral jellyroll tests and simulation.

Fig. 13. Custom designed drop test apparatus (CAD model and actual apparatus).

Table 1
Impact test samples and test conditions.

	Sample orientation	Weight (kg)
Sample 1	Terminals aligned vertically	11.34
Sample 2		22.68
Sample 3	Terminals aligned horizontally	11.34
Sample 4		22.68

points of the experiment and the simulation, the load–displacement curve is started at the time when the inner hole is about to close. Fig. 12 depicts a comparison of the load–displacement from the simulation to the one from the experiment. As the figure suggests, the two curves are in a good agreement, which proves that the material properties derived from the flattened jellyroll experiments are acceptable and can be used for impact simulations.

3. Drop-test lateral impact characterization

3.1. Experimental procedure and setup

A number of standards have been developed and found in the literature to assess the safety aspects of lithium ion battery cells and packs. These standards typically suggest different experiments on batteries that can be categorized as electrical, mechanical or thermal experiments. Crushing, drop test and impact tests are some examples of mechanical tests found in various standards [8,20]. For example, the impact test is used to determine a cell's ability to withstand a specified impact applied to a cylindrical steel rod placed across the cell under test. Most of these experiments are qualitative tests; that is, to pass the tests, the cell or pack may not explode or ignite. However, in this study, dry cells were used instead of cells with electrolyte and no ignition or explosion was possible. The goal was to validate the finite element model, which will be used for impact simulations. Therefore, instead of impact test using a steel rod, simple impact between two rigid plates was performed on the cells. A 2.8-m drop test apparatus (see Fig. 13) was designed and manufactured for this purpose consisting of a bottom steel plate and a moving drop cart capable of adding additional weight. The drop cart was guided in the drop tower using eight roller bearings that ensured straight movement with minimum friction between the cart and the guide bars. A manual winch was used to lift the drop cart to the desired height before release. A high-speed camera was used to capture the impact scene. Because of the asymmetric shape and location of the anode and the cathode cell terminals, two impact configurations were investigated: (1) horizontal and (2) vertical (see Table 1). We investigated cell impact using two different drop carts weighing 11.34 kg and 22.68 kg respectively.

3.2. Lateral impact: drop-test experimental results

The theoretical impact velocity was calculated using the drop height assuming negligible friction and was found to be equal to 7.4 m s^{-1}. In order to measure the actual plate's impact velocity, a set of markers was placed on the drop tower wall in front of the high-speed camera. By measuring the distance the plate moves between two subsequent frames of the recorded movie, the impact velocity of the drop cart was found to be equal to 7.0 m s^{-1}.

Fig. 14 depicts three frames of the cell impact with horizontal orientation of the terminals: before impact, during impact and after impact. Also, a comparison of undeformed and crushed cells is presented in Fig. 15. Various types of battery failures such as electrolyte leakage, short circuiting or activation of a permanent disabling mechanism are likely to occur due to an impact. But the most critical one would be the short circuit between electrodes that may cause a thermal runaway. The cells being dry, it was impossible to measure the voltage and temperature in order to track the internal short circuits and temperature increases. However, it is always a possibility that the terminals will touch causing an external short circuit due to severe deformation.

3.3. Explicit finite element model of lateral impact

An explicit finite element model of a cylindrical cell was developed to simulate lateral impact in LS-DYNA (see Fig. 16). The crushable foam material model was used as the constitutive model

Fig. 14. Lateral impact test (high-speed camera footage).

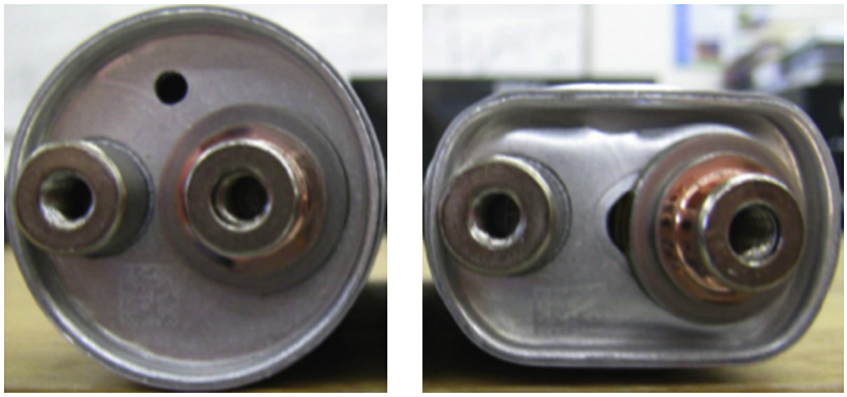

Fig. 15. Cylindrical cell before/and after impact, 11.34 kg drop weight, horizontal orientation.

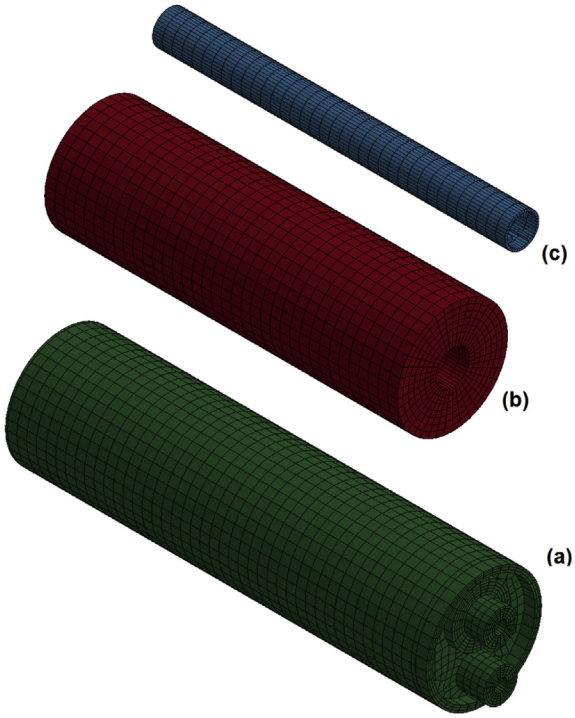

Fig. 16. Main components of a cell's finite element model: (a) case, (b) homogenized jellyroll and (c) inner tube.

for the jellyroll [15], incorporating the stress-strain curve from the flattened tests. The tensile cut-off value of the crushable foam model was set to 10 MPa, based on the tensile strength for coated aluminum, coated copper and separator [17]. The casing and the core tube were assumed to be made of aluminum 1100 (with properties of 99 MPa yield strength and 111 MPa ultimate strength) and modeled in LS-DYNA using material model 24 (Piecewise Linear Plasticity). An internal spacer between the terminals and the jellyroll was assumed to be made of polyetherimide and modeled in LS-DYNA with material model number 3 (MAT_PLASTIC_KINEMATIC) [21,22]. All of the components were modeled using one-point integration solid elements. There were 19,740 elements in the model. Having elements with reduced formulation in the model, hourglass Type 6, Belytschko-Bindeman was used to prevent nonphysical, zero-energy modes [21,22].

The battery cell was placed on a lower rigid plate (see Fig. 17) and crushed by a rigid plate, which was dropped from a 2.78 m height. The impact velocity based on calculations was 7.4 m s^{-1}, and the weight of the rigid plate was set to 11.34 kg and 22.68 kg respectively. Two impact configurations were modeled using LS-DYNA, as depicted in Fig. 17.

Fig. 18 shows the deformed cell shape found through the finite element analysis. In order to compare the results to the experiments and verify the finite element simulation, the dimensions of the deformed cell at three sections (A) top, (B) middle and (C) bottom are listed in Table 2. The first two rows include the values for the cell with horizontal terminals, and the last two rows compares the thickness for the cell with vertical terminals. The difference between the experiments and the finite element results in most cases is less than 5%, especially for the sections B and C that are away from the terminals. Some of the errors can be referred to

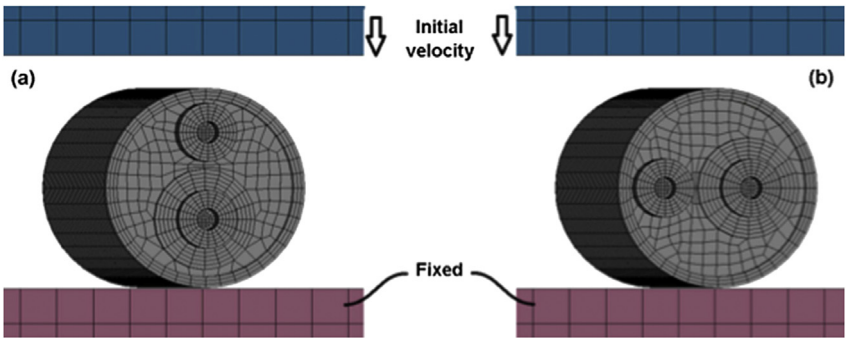

Fig. 17. Cell impact configurations: (a) vertical and (b) horizontal.

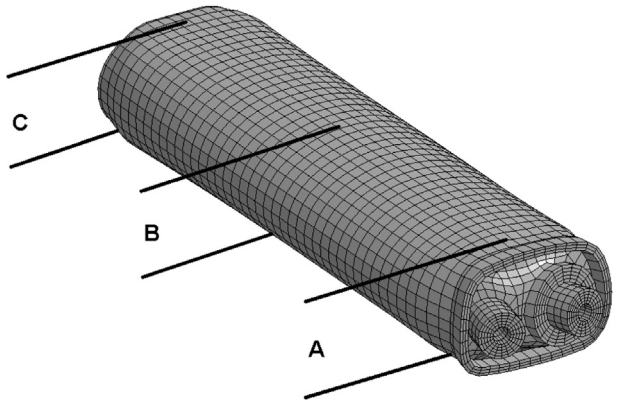

Fig. 18. Deformation comparison locations (horizontal orientation, 11.34 kg weight).

Table 2
Deformed thickness comparison for the cells with horizontal (h) and vertical (v) terminals.

	A (mm)		B (mm)		C (mm)	
	11.34 kg	22.68 kg	11.34 kg	22.68 kg	11.34 kg	22.68 kg
Experiments (h)	30.5	28.4	29.6	27.2	27.5	23.5
FE results (h)	28.2	24.6	28.8	26.1	25.9	23.3
Experiments (v)	29.7	27.8	30.2	27.6	27.0	24.4
FE results (v)	29.4	25.8	30.0	27.4	25.5	23.0

the fact that, in the experiments, the drop cart might not be completely horizontal before the impact.

The jellyroll's stress-strain curve, assuming an isotropic material model, and the skipping rate dependency of the mechanical properties can be other sources of the error. The impact load is plotted over time in Fig. 19 based on the load transferred to the impacting plate. The maximum impact load was found to be 120-140 KN for the 22.68 kg tests and 44-48 KN for the 11.34 kg drop weight respectively. Variation of the plate's velocity over time is also plotted in Fig. 20. During the impact, the velocity changes from 7.38 m s^{-1} in the downward direction to 1.6–2.7 m s^{-1} in the upward direction. From the velocity curve, the impact duration can be estimated to be around 3.7 ms for the 11.34 kg impact and 3.2 ms for the 22.68 kg impacts. Considering the fact that the drop weights

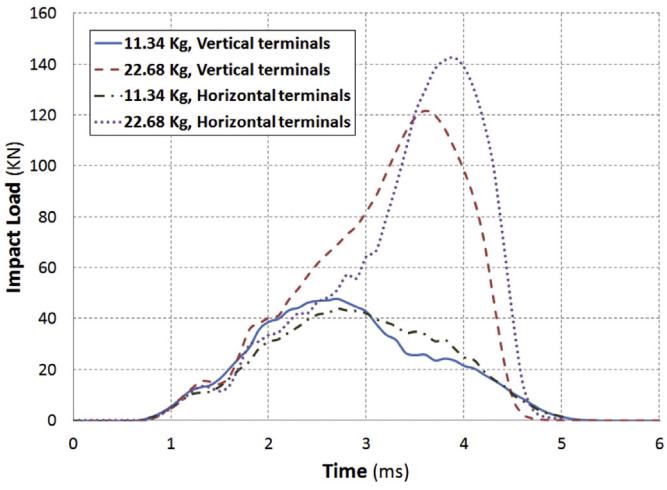

Fig. 19. Impact load for various load cases and cell orientations.

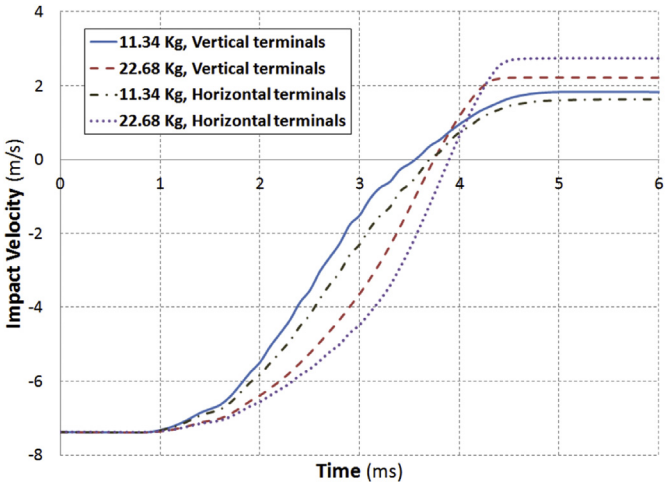

Fig. 20. Impact velocity for various load cases and cell orientations.

are rigid, the mean impact load can be estimated using the plate's change of linear momentum. These average impact force values are calculated using Eq. (12) and are listed in Table 3. This could be another criterion to verify the simulation results, because the average loads match the load variations plotted in Fig. 19. The cell's terminals being in vertical or horizontal orientations slightly changes the maximum impact load, however the average impact force and the impact duration remains the same.

$$F_{\mathrm{av}} = \frac{\mathrm{d}(m_d V)}{\mathrm{d}t} = m_d \frac{V_2 - V_1}{t_{\mathrm{impact}}} \tag{12}$$

In order to find the deformed shape of individual components inside the cell, deformed cells were CT scanned using a 3-D CT scanning system at the Johnson Controls, Inc. battery testing laboratory (Glendale, WI). Fig. 21 compares two cross sections of the cell after impact with 11.34 kg drop weight with the deformed shapes found from the finite element simulation. The thickness of the jellyroll and inner tube was measured at both sections and is listed in Table 4. A comparison of the cell dimensions shows that the overall deformed geometry, and specifically the jellyroll, is in very good agreement with the CT scanned cell.

The deformed shapes and the Von Mises stress contour of the jellyroll and the inner tube are displayed in Fig. 22. Because the impact in this case only included flat plates, the risk of creating a short circuit and the consequent thermal runaway is not as high as the cases including axial impact or impacts including sharp objects [8]. This is because distributed load is applied orthogonally to the plane of the electrodes. Therefore, the only parts of the cell where the short circuit is likely to occur are the areas with high stresses that may cause the separator to fail. Based on the simulation results, the inner parts of the jellyroll close to the inner tube always experience high stresses, and hence, can be assumed to be the jellyroll's critical points.

Table 3
Impact force estimation.

Cell direction	Weight (kg)	Impact time (ms)	Average impact force (KN)
Vertical	11.34	3.7	28.1
Vertical	22.68	3.2	67.8
Horizontal	11.34	3.7	27.5
Horizontal	22.68	3.3	69.3

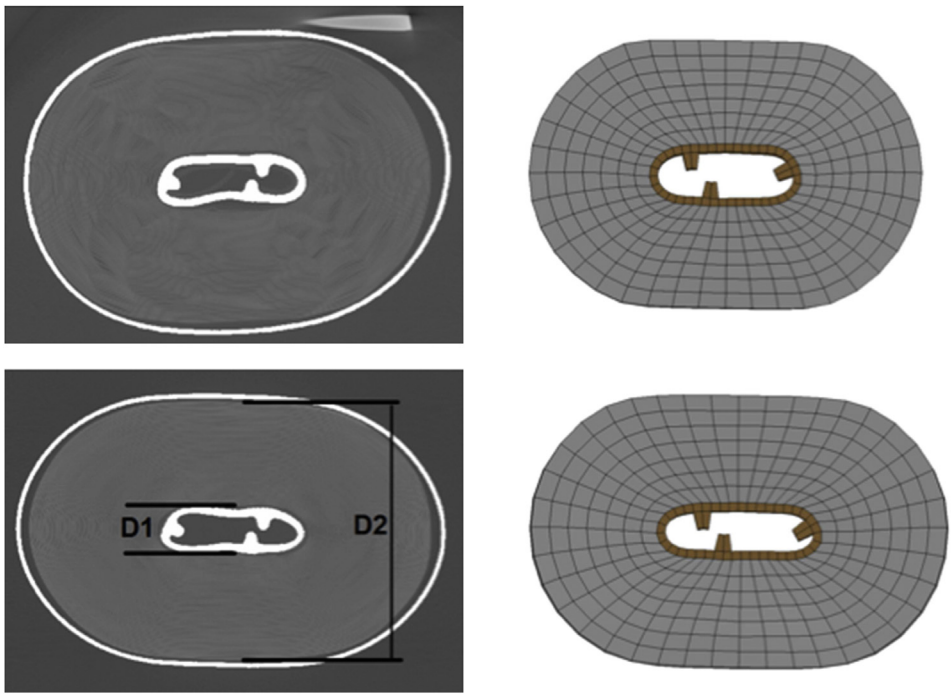

Fig. 21. CT-scan of the cell's deformed shape after impact with 11.34 kg plate (horizontal orientation).

Table 4
Deformed shape thickness comparison of internal components.

	Top cross section (mm)		Bottom cross section (mm)	
	Inner tube (D1)	Jellyroll (D2)	Inner tube (D1)	Jellyroll (D2)
CT scan	4.45	25.19	4.29	24.11
Simulation	5.85	25.00	5.07	24.23

4. Conclusions

We have carried out experimental and numerical characterization of the mechanical response of the cylindrical lithium-ion battery cells used in EV/HEV applications to lateral impact. Highly nonlinear mechanical deformations were characterized experimentally using high-speed camera and computer tomography analysis of the deformed samples. Numerically, we have investigated the feasibility of using explicit finite element code for accurate modeling of impact in one cell as well as in an entire battery pack that consists of hundreds of cells. The following conclusions can be drawn from the results of this study:

1. Two proposed homogenization methods for the jellyroll in a cylindrical lithium-ion battery cell produced similar mechanical response of the homogenized material for relatively small strains. However, for the strains larger than 0.1, the difference between the two material models would gradually increase to be as large as 25% for strains of 0.3.
2. The virtual method homogenization can be accurate for smaller cells, while for larger cells, such as 6P/JCI cells, the direct experimental homogenization using flat samples is the preferred method of determining the effective material properties of the jellyroll.
3. Battery cells were impact tested using a drop test apparatus where a rigid drop cart was dropped onto a stationary cell. Cells were tested using 11.34 kg and 22.68 kg drop weights, each in two orientations where the cell terminals were aligned in vertical or horizontal directions. The experiments showed that these two configurations do not make a lot of difference in the overall deformation of the cells and especially the jellyroll.
4. Based on the results of homogenization, the material model utilizing crushable foam constitutive behavior was then developed for the finite element impact simulations in LS-DYNA. Experimental results showed very good agreement with

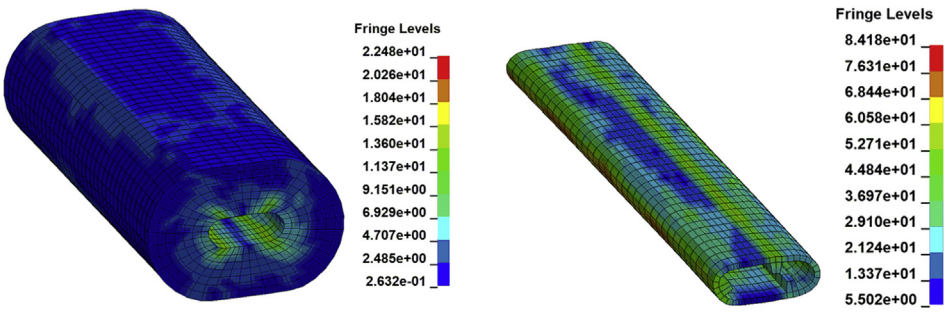

Fig. 22. Jellyroll and inner tube's Von-Mises stress for the horizontal cell (11.34 kg drop weight).

simulations, thus validating the proposed approach and giving us confidence to move forward with the crush simulations of an entire battery pack.

5. A 3-D finite element model of the cell was developed using the crushable foam material model utilizing experimentally obtained effective material properties of the jellyroll. The drop-test explicit simulations were conducted using LS-DYNA. The deformed shape of the cell was in good agreement with the experimental measurements. The impact load and velocity was derived from the finite element analysis, and the impact time was estimated to be 3 and 4 ms for 11.34 kg and 22.68 kg drop tests, respectively.
6. The proposed homogenization methodology coupled with the developed explicit finite element model can be applied to modeling live cells and battery packs subject to lateral impact, which can be used as an effective design tool as well as to give insight into the development of catastrophic response of the EV/HEV battery packs to crash.

Acknowledgments

This project was supported by Johnson Controls, Inc. under research contract MIL106672. The authors would like to acknowledge members of the Advanced Manufacturing and Design Laboratory (AMDL) at the University of Wisconsin–Milwaukee for their contributions. The authors also would like to thank Mr. Paul Frank (JCI) for his help with CT scanning.

References

[1] D.H. Doughty, E.P. Roth, Electrochem. Soc. Interface (2012) 37–44.
[2] S.C. Levy, J. Power Sources 68 (1997) 75–77.
[3] O. Manuel, R.H. Maurer, J. Power Sources 21 (1987) 207–225.
[4] D. Fouchard, L. Lechner, Electrochim. Acta 38 (9) (1993) 1193–1198.
[5] S.W. Eom, M.K. Kim, I.J. Kim, S.I. Moon, Y.K. Sun, H.S. Kim, J. Power Sources 174 (2007) 954–958.
[6] D.H. Doughty, A.A. Pesaran, Vehicle Battery Safety Roadmap Guidance, National Renewable Energy Laboratory, 2012.
[7] P.G. Balakrishnan, R. Ramesh, T. Prem Kumar, J. Power Sources 155 (2006) 401–414.
[8] C. Mikolajczak, M. Kahn, K. White, R.T. Long, Lithium-ion Batteries Hazard and Use Assessment, The Fire Protection Research Foundation, 2011.
[9] M. Chatiri, T. Gull, A. Matzenmiller, in: 7th European LS-dyna Conference, 2009.
[10] J.N. Reddy, Mechanics of Laminated Composite Plates and Shells, CRC Press LLC, 2004. Chap. 3.
[11] I.V. Avdeev, M. Gilaki, in: Proceedings of the ASME IMECE2012, 2012.
[12] S. Kim, Y.S. Lee, H.S. Lee, H.L. Jin, Mat.-wiss. u. Werkst. 41 (5) (2010) 378–385.
[13] L. Greve, C. Fehrenbach, J. Power Sources 214 (2012) 377–385.
[14] E. Sahraei, J. Campbell, T. Wierzbicki, J. Power Sources 220 (2012) 360–372.
[15] E. Sahraei, R. Hill, T. Wierzbicki, J. Power Sources 201 (2012) 307–321.
[16] R. Hill, T. Wierzbicki, Development of a Representative Volume Element of Lithium-ion Batteries for Thermo-mechanical Integrity, 2011 (M.Sc. Thesis, Cambridge, MA).
[17] T. Wierzbicki, E. Sahraei, J. Power Sources 241 (2013) 467–476.
[18] A. Sheidaei, X. Xiao, X. Huang, J. Hitt, J. Power Sources 196 (2011) 8728–8734.
[19] P. Liu, E. Sherman, A. Jacobsen, J. Power Sources 189 (2009) 646–650.
[20] UL 1642, UL Standard for Safety for Lithium Batteries, fourth ed., 2007.
[21] LS-dyna Keyword User's Manual, V971 R6.0.0, 2012.
[22] J.O. Hallquist, LS_DYNA Theory Manual, Livermore Software Technology Corporation, 2006.